Enhancing Mg extraction from lizardite-rich serpentine for CO_2 mineral sequestration

Aimaro Sanna[1]*, Xiaolong Wang[2], Alicja Lacinska[3], Mike Styles[3], Tom Paulson[4], M. Mercedes Maroto-Valer[1,5]

[1] Centre for Innovation in Carbon Capture and Storage (CICCS), School of Engineering and Physical Science, Heriot-Watt University, Edinburgh, EH14 4AS, UK.
[2] China Huaneng Clean Energy Research Institute, Haidian District, Beijing, 100098, China.
[3] British Geological Survey, Keyworth, Nottingham NG12 5GG, UK.
[4] Advanced Materials Technology, Caterpillar Inc. Peoria, IL 61629, USA.
[5] Institute of Petroleum Engineering, Heriot-Watt University, Edinburgh, EH14 4AS, UK.

Corresponding Author: Aimaro Sanna, School of Engineering and Physical Sciences, 3.04 Nasmyth Building, Heriot-Watt University, Edinburgh, EH14 4AS. Tel: +44(0)131 451 3299, E-mail: A.Sanna@hw.ac.uk.

Abstract

Carbon capture and storage by mineralisation (CCSM) is a promising technology that sequesters CO_2 from flue gases into stable mineral carbonates. Although the development of indirect pH swing processes (dissolution at acid pH and carbonation at basic pH) able to recycle the chemicals used are promising, there are still limitations in reaction rate of mineral dissolution being slow in view of a large deployment of the technology. The extraction of Mg from lizardite using magnesium bisulphate has been studied as a function of temperature, reagent concentration, solid to liquid ratio, thermal and mechanical pre-activation. Although the overall highest Mg extraction (95%) was obtained after 3 hours, the reduction of the dissolution time to 1 hr can consistently reduce the volumes to be treated per unit time leading to low capital costs in a hypothetical mineralisation plant. About 80% of Mg was extracted from lizardite in 1hour at 140°C, 2.8 M NH_4HSO_4, particles < 250µm and a solid to liquid ratio of 100g/l. At 140°C, serpentine undergoes extensive structural modifications as indicated by XRD and FTIR analyses, producing amorphous silica and accelerating the kinetics of the reaction. Particles with diameter less than 250µm were obtained by grinding the lizardite at 925rpm for 10 minutes consuming 33kWh/t_{rock}.

Keywords: Clean energy, Mineral carbonation, CO_2 sequestration, serpentine dissolution, serpentine activation

1. Introduction

Currently, the most extensively investigated process for carbon dioxide capture and storage (CCS) is geological sequestration. However, this process is not universally applicable and requires suitable geological formations that are not present in many places or are located offshore and can be uneconomical or impractical (IPCC, 2005). CCS by mineralisation (CCSM) can be used as a potential CCS option, acting as a risk mitigation strategy, where

geological storage might not be practical (IPCC, 2005). CCSM has been identified as a safe and permanent CCS option, and is based on the accelerated reaction of CO_2 from industrial flue gases with Mg-rich silicate rocks or inorganic wastes to form stable magnesium carbonates (Seifritz, 1990). Since industrial wastes seems to be able to sequester only a low fraction (<5%) of the total CO_2 required to fulfil the Kyoto protocol objectives due to the limited volumes available, mineral carbonation of silicate rocks including mines tailings will be essential for the success of the technology (Sanna et al., 2012a; Vogeli et al., 2011). Furthermore, mineral carbonation is well suited for integration in mining operations (Hitch and Dipple, 2012). The natural weathering of rocks is exothermic and thermodynamically favoured at ambient temperature, so that the reaction of Mg/Ca-silicates with CO_2 proceeds spontaneously, although it requires geological times. This is related to the kinetically unfavourable extraction of alkaline ions (Ca, Mg) from the silicate resources under ambient conditions. This unfavourable "extraction" can be accelerated by (i) directly increasing the pressure and temperature of the process or, (ii) indirectly, by using aggressive leaching agents. Although significant research has taken place over the last 20 years on direct processes, they still present poor economic and technical viability on a large scale due to the low reaction rate, long residence time, high pressure and temperature required for the reactions to happen (IPCC, 2005; Gerdemann et al., 2007). Alternatively, the indirect processes show promising results in addressing the low reaction kinetics by the use of additives able to extract the reactive Mg and Ca from silicate rocks that then react fast with CO_2 forming carbonates at mild conditions, but unfortunately large quantities of chemicals need to be recycled (Nduagu et al., 2012a, 2012b).

Among the indirect mineral carbonation routes, the pH swing processes allows the separation and recovery of pure products (e.g. carbonates, silica, and metal oxides) that could be potentially reused in a wide range of sectors, reducing the emissions related with fresh

materials production (Sanna et al., 2012b; 2012c). Also, this group of processes could help in lowering the costs of CO_2 sequestration technology by reducing the precipitation of "silicates impurities" (e.g. Fe, Al) on the surface of the Mg bearing particles, which causes the 'CO_2 diffusion limit' typical of this technology (Teir et al., 2009). CCSM via the indirect pH swing, in the presence of NH_4-salts has recently been investigated resulting in a "slow and limiting" dissolution step that requires about 3hours to reach 80-100% efficiency using antigorite [$(Mg,Fe)_3(SiO_5)(OH)_4$]; followed by a fast carbonation step (~15-30 min) with efficiency of ~90% (Park et al, 2004; Eloneva et al., 2012; Kodama et al., 2008; Wang and Maroto-Valer, 2011a, 2011b; Sanna et al., 2012d). The main advantage of these methods is the recyclability of the chemicals used during the process, which would consume about 300 kWh/tCO_2 and also allow CO_2 capture from flue gas, avoiding additional separation and compression stages (Kodama et al., 2008). Previous work found that the reactivity in mineral carbonation of antigorite and lizardite is very different; with antigorite having a carbonation efficiency of 92% and lizardite [$(Mg,Fe)_3(SiO_5)(OH)_4$] of only 40% after thermo-activation (Gerdemann et al., 2007). This suggests that the mineral phase used as resource is an important aspect to evaluate a potential CO_2 sequestration technology. So far, lizardite, which is the most common and readily available serpentine species in the UK, has not been tested using the ammonium-based pH swing process (Maltman, 1977; Cressey et al., 2008).

A cost sensitivity analysis of the ARC/NETL mineral carbonation process based on 95 reactor vessels able to treat 24 kt CO_2/day, found that the cost of the carbonation reactors, which represented about 70% of the overall costs, would decrease from ~£620M to ~£310M (50%) if the residence time in the reactor were decreased from 2 to 1 hour (White, 2003). This indicates there is potential to reduce capital cost through better reaction understanding, coupled with an improved design approach. Faster dissolution kinetics can lower the costs of the NH_4-based pH swing carbonation technology, since the dissolution represents the longest

and limiting step (3 hrs) compared to the carbonation step, which has a efficiency of 90% after 30 minutes (Wang and Maroto-Valer, 2011b). Therefore, in this study, further research is conducted on the NH_4-salts pH swing process with the objective to optimise the lizardite dissolution variables (temperature, particle size, solid to liquid ratio, residence time) using ammonium bisulphate to enhance the potential for large-scale deployment of this technology.

Thermal activation of serpentines can be described as a thermo-chemical decomposition reaction of the parent minerals to form a so-called "meta-serpentine" phase while releasing water from the crystal structure (McKelvy et al., 2004). It was demonstrated that the kinetics of the mineral dissolution and aqueous carbonation steps increases by almost an order of magnitude after heat activation of serpentine at 630°C for 2 h in a direct mineral carbonation processes, resulting in an energy requirement of 326 kWh/t of lizardite treated (O'Connor et al, 2005). The effect of thermal-activation at a lower temperature and shorter time needs to be evaluated to establish its influence on the Mg-extraction using a pH-swing process and to establish the potential energy consumption reduction. Mechanical activation renders the crystal lattice of minerals less stable and this "disorder" contributes to lowering the activation energy for any further reaction of the material, such as chemical dissolution or CO_2 adsorption (Tromans and Meech, 2001; Fabian et al., 2010). Previous work indicated that increasing the milling energy input increased the materials amorphisation (Pourghahramani and Forssberg, 2006). The effect of short time at high speed and in presence of flue gas may reduce the energy consumption of grinding serpentine to a particle size needed to extract high level of Mg from the mineral lattice for the following carbonation reaction. This needs to be evaluated using the NH_4-salts pH swing process.

2. Materials and methods

2.1Experimental summary

This study aimed to investigate the parameters that can affect the Mg extraction from a silicate rock, namely serpentinite. A serpentinised lherzolite from the Lizard peninsula, Cornwall, UK was selected for the optimisation study. This rock contains ca 98% of serpentine minerals, ca 2% of hematite and a trace amount of calcite. The serpentine is a mixture of the two polytypes of lizardite (1M and 1T) and is different in composition in this respect to those used in previous work, which were richer in the antigorite type (Wang and Maroto-Valer, 2011a; Sanna et al, 2012d) . A series of dissolution experiments were performed in a batch reactor using the same serpentinite rock but at different temperatures, particle sizes, NH_4HSO_4 concentrations, different solid to liquid ratios and different pressures. Also, the effect on the Mg-extraction of two different pre-treatments were investigated, namely thermo-activation and fine grinding. A summary of the investigated parameters is presented in Table 1.

2.2 Chemical Activation

The experiments on the optimisation of serpentine dissolution were carried out by placing 20 g of serpentinite into a three neck flask glass reactor containing 200 ml of NH_4HSO_4 solution with a constant stirring rate of 800 rpm and heated using a silicon bath at the desired temperature, as reported in previous works (Wang and Maroto-Valer, 2011a, 2011b). The dissolution experiments at 140°C were carried out using a 0.5 litre stainless steel Parr reactor (model no. 4575A). An aliquot of 1 ml was extracted after 5, 10, 15, 30, 60, 120 and 180 min to determine the content of Mg and other ions in the solution. After 3 h of dissolution, the flask content was cooled down to ambient temperature and filtered with a 0.7 μm Pall syringe filter. After the dissolution experiments, the majority of elements other than Mg were removed as hydroxides by adding ammonia-water. This raised the initial acid pH of the solution from 0-1 to a pH value of 7 to precipitate all the impurities such as iron, manganese, nickel and aluminium. Then, 1 ml of solution was acidified with 2 ml of 70% HNO_3 (trace

metal grade, Fisher Scientific) and then diluted to 100 ml with deionised water to be analysed by Inductively Coupled Plasma Mass Spectroscopy (ICP-MS). A Thermo-Fisher Scientific X Series Instrument, was used to measure the concentrations of the dissolved Mg, Fe and others elements in the samples as in previous work (Sanna et al, 2012d). Fourier Transform Infrared Spectroscopy (FTIR) was performed using BioRad Excalibur spectrometer system that includes a PC-based data system and the optical bench. The optical bench contains a 60° dynamically aligned Michelson interferometer with ceramic infrared source, an air-cooled Deuterated Tri Glycine Sulfate (DTGS) detector and potassium bromide beam splitter. The analysis was performed on KBr discs (1% dilution), using 60 scans and 2cm^{-1} spectral resolution. The morphology and elemental composition of the serpentine before and after chemical activation at 140°C was determined by SEM-EDS analysis. The Scanning Electron Microscopy used was an FEI Quanta 600 (Tungsten filament). Phase/mineral identification was aided by observation of energy-dispersive X-ray spectra recorded simultaneously during SEM observation, using an Oxford Instruments INCA 200 energy-dispersive X-ray microanalysis (EDS) system.

2.3 Mechanical Activation

An attrition mill with a water cooling jacket (model 01HD from Union Process Inc.) was used for the serpentine mechanical-activation with yttrium zirconium oxide as milling media (grinding media to process mineral ratio of 20:1). Both 5 mm and 10 mm diameter grinding media spheres were used, with a mass ratio of ~1:3 (5 mm/10 mm). Total solid mass was approximately 1140 g for each run. The particle size distribution was determined and an average mass loss of 3 wt% was found. Grinding in simulated flue gas was performed by connecting the gas line from gas mixture cylinder to the gas/fluid injection port at the bottom of the grinding chamber. A gas outlet port was located on the top of the grinding chamber and was connected to the absorbing neutralising aqueous media through flexible tubing. X-

ray diffraction analysis was performed using a Brucker D8 diffractometer; 2θ range from 11.22 to 12.87 was selected for automatic peak area measurement of the characteristic 1T lizardite peak for all samples. A micrometrics ASAP 2020 was used for BET measurements by degassing ~0.5 g of sample at 350°C for 4 h. Power draw (as current and voltage) was recorded directly from the motor during grinding using a data logger.

2.4 Thermal Activation

About 2 g of serpentinite were used for heat treatment experiments. After grinding, powder samples were placed in alumina crucibles such that the thickness of the powder bed was ~5 mm. To avoid the temperature overshot, the heating ramp was first set at 30°/min up to 580°C, and after that, at 10°/min up to 610°C. After 30 min of dwell time, the heating was turned off and mineral samples were removed from the oven for quick cooling at ambient conditions.

3. Results & Discussion

3.1 Chemical Activation

3.1.1 Effect of temperature

The effect of time and temperature on the Mg extraction from the lizardite-rich serpentinite sample was investigated and the results are presented in Figure 1. It can be seen that temperature has a significant effect , where the higher temperatures of 100, 120 and 140°C produce much higher Mg extraction efficiency (after 3hours) than the lower temperatures (Figure 1). At 100°C and 60 min dissolution, 1.4 M NH_4HSO_4 was able to extract 60% of Mg, while less than 30% were removed at 70°C. The Mg extraction from lizardite was lower compared to that obtained from the USA antigorite used in previous experiments, where 80% and ~100% Mg was extracted in 1 and 3 hours, respectively (Wang and Maroto-Valer, 2012).

Therefore, lizardite, which represents the main UK resource for mineral carbonation, requires higher temperature to extract a reasonable amount of Mg. The experiment carried out at 140°C indicates that the Mg extraction efficiency is enhanced in the first hour of dissolution (67% Mg extracted) compared to the extraction at 100°C. This is comparable to the highest extraction of Mg from high energy penalty roasting of serpentine and ammonium sulphate at 440°C for 1 hr (Nduagu et al., 2012a, 2012b). Also, this decreases the residence time of the slurry into the reactor, which can reduce the costs associated to the reactors number/size. This higher temperature could not be achieved using the 3-neck glass flask used for the other temperatures due to the evaporation of the water solution from the increase in pressure. Therefore, the experiment was carried out using a 0.3 L Parr high pressure reactor using the same procedure. The final pressure registered at 140˚C was 4 bar.

The effect of temperature on the structure of the serpentine samples is clearly depicted by FTIR analyses. Figure 2 shows absorbance spectra of serpentine, dissolution residues obtained at 100°C and 140˚C and an amorphous silica standard. Spectrum (d) is typical of highly polymerised amorphous silica (Loring et al., 2011). The very strong and broad band at 1105 cm^{-1} with a shoulder towards higher wavenumber is assigned to the Si-O-Si asymmetric stretching vibrations, and the band at 800 cm^{-1} can be assigned to Si-O-Si symmetric stretching vibrations (Musić et al., 2011). The broad band at around 3430 cm^{-1} and low intensity peak at *ca* 1630 cm^{-1} arise from stretching and bending vibrations of H_2O molecules respectively.

Spectrum (a) shows the starting serpentinite. The peak around 960 cm^{-1} is assigned to the Si-O basal vibration, while the lower intensity peak at about 1080 cm^{-1} is characteristic of the Si-O apical vibrations. The peak at 613cm^{-1} is probably related to in-plane displacement of H atoms (Balan et al., 2002). The sharp peak at 3688 cm^{-1} reflects OH bonded to Mg cations in the octahedral position. This peak is characterised by asymmetry towards the lower energies

with a distinctive shoulder occurring at *ca* 3650 cm^{-1}. The asymmetry is interpreted as a slight variation of O-H bond strength, possibly arising from heterogenic cation substitution in the predominantly Mg-dominated octahedral site (Fuchs et al., 1998; Mellini et al., 2002).

The spectra of dissolution residues b (100°C) and c (140°C) clearly indicate a change in the reactants` structure after the dissolution treatment. Starting with the most prominent peaks in the Si-O spectral range the residues show a low intensity peak at *ca* 796cm^{-1} that although slightly shifted, could correspond to 802cm^{-1} peak in the silica standard (symmetric stretching of Si-O-Si). Peaks at approximately 960cm^{-1} coincide with the position of Si-O basal vibration that is clearly seen in the starting serpentine material. The intensity of this band noticeably decreases with the temperature of dissolution (Fig. 2, red arrows).

At higher wavenumber region, the reaction residues display two well defined peaks, one at *ca* 1090 cm^{-1} and other at 1145 cm^{-1}. Assignment of these bands is ambiguous and it is probably a combination of a portion of Si-O apical vibrations originating from the starting serpentinite as well as asymmetric Si-O-Si stretching bands of the newly formed silica. The minor peak shift from 1105cm^{-1} in the silica standard to lower wavenumber in the reaction residues 1094 and 1089cm^{-1} for (100°C) and (140°C) respectively, could be related to subtle structure variation (e.g. newly formed silica). Crystallinity of quartz was previously identified by a band at 1145 cm^{-1}, and this band is observed in our reaction residues (Shoval et al., 1991).

Better defined peaks indicate well-crystallised quartz, and conversely the poorly defined shoulder, as observed in the analysed silica standard is indicative of low crystallinity. Whether the silica formed in our experiments is crystalline, primary amorphous or a combination of both requires further investigation; the XRD data suggest a predominant amorphous component that is consistent with the peak heights in the FTIR spectra. This is an important aspect in terms of utilisation of the produced silica, since amorphous silica is a

desired additive for cement. The reaction residues also display low intensity peaks (Fig 2, green arrows) at around 625cm^{-1}, humps at 745cm^{-1} and three more peaks around 1430cm^{-1}, these bands are probably related to newly formed hydrated NH_4 and/or Mg sulphates, by-products of the experiment.

At the far end of the mid-infrared region (3000-4000cm^{-1}), the reaction residues show a distinct broad band between 3000-3600cm^{-1}. These bands, due to poor resolution and possible overlaps are probably related to a combination of infrared absorptions by various phases present in the samples analysed. The indistinct humps at *ca* 3250 cm^{-1} and 3400 cm^{-1} could however be related to stretching vibrations of Si-OH groups in the structure of amorphous SiO_2 due to bonded water and stretching vibrations of H_2O molecules (Musić et al, 2011).

The effect of temperature on the serpentine structural modifications can be observed in the XRD traces (Figure 3), where it can be seen that the crystal structure of the lizardite-rich serpentine remains almost unchanged after dissolution at 100°C (Figure 3-b), compared to the starting serpentine (Figure 3-a). On the contrary, Figure 3-c shows that the serpentine undergoes extensive structural modification as indicated by significant peak broadening. This suggests that the starting material has undergone amorphisation during the 140°C experiment. The resulting amorphous material is readily dissolvable.

SEM images of the untreated serpentine particles and the reaction residuum after the dissolution at 140°C are shown in Figure 4. Four different particle-types were identified and their elemental composition analysed. Particle 1 (Figure 4-a), represents the average serpentine particle with size ranging from 75 to 150µm. As shown on the EDX spectrum, the particle is composed of the expected Mg, Fe, Al, Si, O. The dissolution residue obtained at 140°C contains chemically different particles. Overall, three compositional types were

observed (i) particles rich in Si and virtually free of Mg (Figure 4-b-2); (ii) particles poor in Mg and rich in Si (Figure 4-b-3); and (iii) particles poor in Mg, rich in Si and S. Particle 1 resembles the elemental composition of lizardite. Particle 2 suffered a strong chemical modification becoming silica-dominated, while particle 3 suffered a lower level of transformation that may be related to the different starting mineral phases (difference between L-1T and L-1M). Both particles 2 and 3 present some sulphate impurities on surface. Instead, the distribution of Mg, S, O and Si in particle 4 indicates that it is probably made of a mixture of partially dissolved serpentine and Mg sulphates. The Mg:S ratio indicates that the sulphate phase could be epsomite (9.8% Mg, 137% S, 71% O), which has the following chemical formula $MgSO_4 \bullet 7(H_2O)$. This is supported by the XRD of dissolution residue shown in Figure 3-c. The Mg-sulphates formed due to precipitation of the excess NH_4-salts used in the experiment.

3.1.2 Effect of additive concentration

Previous work indicated that the concentration of the leaching agent is an important parameter to enhance the cations extraction, since this can accelerate the reaction kinetics and decreasing the residence time of the slurry into the reactor (Wang and Maroto-Valer, 2011a; O'Connor et al, 2005). Accordingly, a series of experiments were conducted to evaluate the effect of the leaching agent concentration (1M, 1.4M, 2M and 3M) on the Mg extraction from lizardite-rich serpentine, and the potential for shortening the reaction residence time. The results shown in Figure 5 indicate that a 1M NH_4HSO_4 solution can extract only 60% of Mg after 3h dissolution, while a 1.4M solution can remove 60% after 1h dissolution and 76% after 3h. Therefore, a long reaction time is required for the serpentine dissolution in presence of 1M and 1.4M NH_4HSO_4 solution. To reduce the dissolution reaction time while maintaining an acceptably high Mg extraction of 70%, a 2M NH_4HSO_4 solution is required for a 1h extraction period. The 3M NH_4HSO_4 solution was the most effective extracting 80%

Mg in just 1h. The effect of NH_4HSO_4 on the extraction of Fe, the main "impurity" element in the serpentine used, is reported in Table 2. Clearly, the stronger the salt solution, the stronger is the removal of Fe from the mineral lattice, i.e. 2M and 3M NH_4HSO_4 solutions are able to extract 100% of the Fe from the serpentine particles after 120 minutes dissolution. Much of the Fe is as Fe^{2+}in the serpentine mineral structure but some is present as Fe^{3+} or mixed valences in magnetite, hematite and chromite. Chromite and magnetite are known to be resistant to leaching and require strong leaching solutions and high temperature/pressure (Liu et al, 2010; Vardar et al, 1994). Magnetite was found attached to the magnetic stirring bar after the experiment. The leached impurities can be separated from the main solution stream of $MgSO_4$ by precipitation of Fe hydroxides. Therefore, the concentration of the leaching agent is a primary player if we want to maximise the extraction of all the other cations (apart from Mg) from the mineral lattice. This will leave behind pure amorphous silica that has a potential application in the construction sector as cement additive. Therefore, working at concentration $\geq$ 2M NH_4HSO_4 at 140°C will produce a dissolution residue predominant in amorphous component as confirmed by the XRD and FTIR analyses in Section 3.1.1.

3.1.3 Effect of particle size

The dissolution results using different particles sizes are shown in Figure 6 and indicate that the particle size has a large effect on final extraction of Mg from the mineral lattice.

The dissolution of the sample with the larger particles (500-700µm) was not successful giving only 30% and 60% Mg, respectively after 1h and 3h of extraction. In contrast, the dissolution carried out at the smallest particle size (< 75µm) gave 70% and 90% Mg extraction after 1h and 3h dissolution. When particles with size less than 300µm were used, the Mg extracted was about 60% for 1h dissolution and 80% after 3h. This shows that the improvement in Mg extraction is big from reducing from 500µm to 300µm, but much less

going from 300µm to <75µm. However, the energy required to grind the serpentine to <75µm shows a substantial increase. Besides, particles larger than 500µm would require a long extraction time and particles < 75µm would consume too much energy. All grinding processes, particularly on an industrial scale produce a significant amount of undersize fine material. Grinding to produce a particle size less than 300µm will inevitably create a lot of material with a much finer particle size, so that particles < 250µm instead of defined particles range such as 75-150µm will represent a realistic case, which is treated in Section 3.2.1.

Interestingly, the particles mixture with about 40% of <75 µm, could liberate some of the magnetite from the serpentine mineral, partially eliminating the need for a large Fe removal step in the overall process (Lackner et al., 2008). The Mg extraction improved by about 10% using particles < 75 µm compared to particles between 75-150 µm between 30-60 min dissolution. Logarithmic trends have been used to predict the total time required to extract the majority of Mg from the serpentine using very small <75µm particles and particles in the range of 75-150µm. Figure 7 shows that the logarithmic trend has a good fit with the experimental data, with an R^2 close to 1 in both the cases. About 6 hours would be required if particles <75 µm are employed, while the dissolution will be lengthened to 10 hours when the larger particles are used. The physic-chemistry meaning of having a parabolic trend can be explained with two different dissolution mechanisms, an initial stoichiometric dissolution of the external layers of serpentine followed by a non-stoichiometric extraction of Mg with transport in the solid resulting as the dissolution controlling mechanism (Brantley et al., 2003). Previous work on olivine indicates that a 50 nm thick altered zone depleted in cations and enriched in Si has formed (Béarat et al., 2006). The FTIR (see Figure 2) and SEM-EDS (Figure 4) analyses of serpentine indicate that the dissolved residues are richer in silica compared to the starting serpentine and this can be related to the parabolic trend shown in Figure 7. The particle size of the serpentine fed to the dissolution stage has also an important

effect on the extraction of the other elements in the mineral matrix as reported in Table 3. The dissolution of particles reduced to <75μm in presence of mild NH_4HSO_4 (1.4M) is able to extract 100% of Fe in 2 hours and more than 90% in just 1 hour. However, less than half of the Fe is removed when larger particles are used.

3.1.4 Effect of solid to liquid ratio

The solid to liquid (S/L) ratio is an important parameter in terms of capital and operating costs because working at high S/L ratios reduces the volumes treated in unit time and consequently lowers the number of units or size of the single unit employed in the process. For example, to capture 1MtCO_2/y using 3t of serpentine per t CO_2 captured, about 6800 t_{slurry} or 3400 t_{slurry} would need to be processed each hour, using a solid to liquid ratio of 50 g/l or 100 g/l, respectively. This would consistently decrease the capital costs due to a low number of reactors required in the process. Previous work indicated that using S/L ratios of 200 or 300g/l in the NH_4-salts process reduces the dissolution efficiency from 100% to 65-70% in 3 hours time using antigorite-rich serpentine, due to the precipitation of $MgSO_4$ at S/L ratio higher than 180g/L (Wang and Maroto-Valer, 2013).The results of our study using 25, 50 and 100g/L at 100 and 140°C, indicate that a S/L ratio of 100g/l using 2.8M NH_4HSO_4 at 140°C can extract 72% of Mg in 60 minutes, when particles between 75 and 150μm are used. If particles <250μm and slightly concentrate NH_4HSO_4 solutions are used, the Mg removed can be increased to ~80-85%. This percentage can further be enhanced to 90% at 140°C just after 15 minutes using an S/L ratio of 25g/l, but with any advantage from the costs point of view. Therefore, S/L ratio between 100g/l and 180g/l can be used to extract Mg during the serpentine dissolution at 140°C. The use of 100 g/l serpentine to NH_4HSO_4 solution ratio can decrease by half the volumes to be treated in the dissolution stage compared to 50g/l. Also, the use of a high S/L ratio would lead to an improved heat balance, due to less energy

required heat the reactor, reduced size of the reactor and less energy required to pump the slurry (Huijgen et al., 2006).

3.2 Pre Chemical activation treatments

3.2.1 Effect of mechanical activation

Since grinding to produce a particles < 300μm will inevitably create a lot of material with a much finer particle size, some grinding experiments were carried out to establish real particles distribution and energy consumption. The following particle size distribution was produced in a single run using starting feed mineral of 5 mm after 10 minutes: 38% of milled material with particles diameter < 75μm, 50% 75-150μm, 1% 150-250μm and 11% > 250μm. The particles with diameter < 250μm decreased to 55% after only 5min grinding at 925rpm. The <250μm particles were tested in a dissolution experiments to compare the Mg extraction with standard 75-150μm particles and thermo-activation (see following section). Grinding for 5 min at 925rpm allowed to extract 5% more Mg compared to the standard experiment, as can be seen in Figure 8. However, it is expected that the percentage of Mg removed from the serpentine grinded for 10 min will be higher (+10%), since 88% of the particles are <150μm, compared to the material grinded for only 5 min. However, the experiment to confirm it was not run. Table 4 shows the Particle Size Distribution (PSD) and energy consumption (kWh/t) after grinding at increasing mill speeds and different times. To make mechanical activation of minerals attractive, the energy used for activation has to be minimised. In this study it was found that the use of a shorter grinding time (5-10min) at higher speed (925rpm) is able to produce 55%-88% particles < 250μm consuming 17 and 33kWh/t rock, respectively in 5 and 10 minutes. This consumes less energy than longer duration at slower speeds (314/409rpm - 60 min) requiring 69-87kWh/t_{rock}. The highest mill speed also produced the largest fractions of particles with diameter < 250μm and <150μm. It has been reported that grinding in presence of pure CO_2 improves the follow up carbonation reaction (Nelson, 2004). Therefore,

a set of grinding tests was performed in hot air (100°C) and hot simulated flue gas mixture (100°C, 10% CO_2, 5% O_2, 3000 ppm SO_2, 500 ppm CO, 250 ppm NOx, N_2 balance) and their effect on the crystalline structure of serpentine (Cxrd) detected by XRD can be seen in Figure 9. The results showed that about 40% of the starting crystalline structure was destroyed by grinding the serpentine in presence of flue gas, while only 10% of the structural bonds were removed by grinding in presence of air. Therefore, enhanced leaching of Mg from silicates can be obtained in presence of flue gas by breaking the structural bonds and producing amorphous material. Based on the experimental data, grinding can be performed for a short time and at high rotation speed to produce a large fraction of < 250μm. Also, the presence of hot flue gas resulted in additional amorphisation of minerals, but it would require expensive gas tight grinding equipment. The results confirm that a particles mixture < 250μm can be successfully employed to extract Mg from serpentine with a small associated energy penalty and that using the fines produced at no extra cost a further 5-10% Mg is extracted, compared to experiment using 75-150μm at 100°C and 1.4M NH_4HSO_4.

3.2.2 Effect of thermal activation

The thermal-activation experiments in this study were performed for 30 minutes at 610 °C requiring 245 kWh/t_{rock} instead of 326 kWh/t_{rock} required for the dehydroxylation at 630°C for 2 hours, where 206 kWh/t (Cp=89.26 cal/K*mol, dT=605°C) were used to heat lizardite to the target temperature and 120 kWh/t were used to keep the dehydroxylation temperature for 2 hours (Gerdemann et al., 2007; O'Connor et al, 2005). Previous studies indicated that heat treatment in pure CO_2 gas could also improve the kinetics of the follow up aqueous dissolution-carbonation steps (Dahlin et al., 2000). In this study, a simulated flue gas mixture was used (10% CO_2, 5% O_2, 3000 ppm SO_2, 500 ppm CO, 250 ppm NO, N_2 balance) instead of pure CO_2, but no measurable changes in mineral amorphisation were observed when a flue

gas was used during thermal-treatment. The thermal-activated and mechano-activated serpentinites were tested in the dissolution experiments at 100°C to compare the Mg extraction with the chemical activation option and the results are displayed in Figure 8. Various functions were applied to fit the data including linear, logarithmic, and power; the best data fit was achieved with the power functions (%Mg~(LogT)^{n}), shown on the plot. Based on the experimental data discussed above, ~75% Mg is extracted from the standard 75-150μm serpentine after 60 minutes. Mechanical activation (5 min at 925 rpm) increases the Mg extraction to 80%, while a larger fraction of Mg (90%) is removed from serpentine after just 10 min of dissolution of thermal-activated serpentine. The Mg extracted resulted higher compared to previous work where thermal activation at 640-700°C for 1 hr (Fedoročková et al., 2012). Therefore, thermo-treatment is more effective in accelerating the Mg extraction, but with high associated energy penalty, while mechanical pre-treatment is able to increase the Mg extraction in the following dissolution with low energy penalty (17-33 kWh/t rock used).

3.3 pH swing and carbonation steps

The second stage of the overall process is the pH swing step, from acidic (pH between 0 and 2) to neutral (pH 7), by the addition of ammonia water. This is to remove all the impurities (Fe, Al, Ni, Mn etc.) from the solution by precipitating them mainly as hydroxides. These hydroxides may be used for the production of pigments or as iron ore feedstock for the steel and iron industry (Sanna et al., 2012b). Table 5 shows the concentration of Fe, Al, Ni, Mn and Mg as a function of the pH change. Even if ICP-MS is a very good technique to analyse traces of elements, the concentration of Al, Ni and Mn might present an error due to their very low content (< 1wt%) in the starting serpentine. At the final pH value of 7, more than 95% of Fe and Al are removed from the solution, while only 55% of Ni and 28% of Mn are precipitated at the end of the process. About 3% of Mg was lost from the solution during the

pH swing process, leaving a solution rich in $MgSO_4$ ready for the carbonation reaction. After the pH swing process, the Mg-rich solution is carbonated by reacting it with ammonium bicarbonate (NH_4HCO_3) obtained from the capture step by reacting ammonium hydroxide (NH_4OH) with the flue gas (Wang and Maroto-Valer, 2011b). The product of the reaction under the used conditions is hydromagnesite, which may access niche markets to produce high-value fillers (e.g. paper filler) (Sanna et al., 2012b). Also, it could be used (together with the hydroxides from the pH swing step) to produce low value controlled low-strength materials, which represent a solidified geotechnical composite for fill application (Bouzalakos et al., 2008). The efficiency of the carbonation reaction can be represented by the precipitation of Mg from the solution in the form of hydrated carbonate (Table 6). After 60 minutes reaction, only 6 wt% of Mg did not react with the ammonium bicarbonate salt. Also, ca 77 wt% of Mg precipitated in just 10 minutes. Therefore, in a real carbonation plant, a residence time of the slurry into the precipitator of 10 minutes would be preferred to minimise the volumes to be treated in the unit time by maintain a good efficiency (77% Mg to carbonate) and consequently lower the capital costs of the plant.

4. Conclusions

The objective of this study was to optimise the dissolution of a lizardite-rich serpentine in order to facilitate the large-scale deployment of this technology. A set of dissolution conditions (temperature, particle size, solid to liquid ratio, reagents concentration) and two different pre-treatments (mechano- thermal- activation) were investigated.

The maximum extraction of Mg (95%) from the serpentine lattice was achieved after dissolving 50g/l of a thermal-activated lizardite for 3 hours at 100°C. Besides, the dissolution conditions were optimised to maximise the extraction of Mg in a shorter time, since this can consistently reduce the volumes to be treated and thus leading to a lower capital expenditure.

An average of 80% of Mg was extracted in 1 hour when using a temperature of 140°C, and 2.8 M NH_4HSO_4, particles < 250μm and a solid to liquid ratio of 100g/l. Using 100g/l would reduce the slurry volumes of a theoretical 1MtCO_2/y plant from 6800t/h to 3400t/h. Moreover, the shorter dissolution residence time (1hr) would further reduce the number of reactors to be employed. The temperature plays an important role in accelerating the dissolution of lizardite as depicted in the FTIR spectra and by the broadening of XRD peaks.

The reactivity of different minerals, including polymorphous minerals can change significantly the reactions condition and reactors design, as found in this work, and therefore, resource evaluation is a critical aspect to take into account during the techno-economic assessment of ex-situ mineral carbonation processes.

A mechano-activation process to grind the serpentine at 925rpm for 10 minutes was able to produce particles with size < 250μm, which helped dissolving 80% of Mg in 1 hour at a reasonable energy penalty of 33 kWh/t rock. Addition of CO_2 during the mechanical activation helped in destroying the crystallinity of the mineral, and therefore extracting more Mg from the mineral, but this would require expensive gas-tight equipments. Instead, thermal-activation at reduce temperature and time (610°C, 30 min) compared to previous work, helped to completely dissolve lizardite, but the associated energy penalty (250 kWh/trock) remained significantly high.

5. Acknowledgements

The authors thank the Energy Technologies Institute (ETI) that commissioned and funded the work as part of its CCS programme. Also, the authors thank the Centre for Innovation in Carbon Capture and Storage, Heriot-Watt University (EPSRC Grant No. EP/F012098/2) and Svetlana M. Zemskova, Advanced Materials Technology, Caterpillar Inc, for the mechano-activation work. AML and MTS, publish with permission of the Executive Director of the British Geological Survey (NERC).

6. Reference

Balan, E., Saitta, M.A., Mauri, F., Lemaire C. and Guyot F., 2002. First- principles calculation of the infrared spectrum of lizardite. Am. Mineral. 87, 286-1290.

Béarat, H., McKelvy, M.J., Chizmeshya, A.V.G., Gormley, D., Nunez, R., Carpenter, R.W., Squires K. and Wolf, G.H., 2006. Carbon Sequestration via Aqueous Olivine Mineral Carbonation: Role of Passivating Layer Formation, Environ. Sci. Technol. 40, 4802–4808.

Bouzalakos, S., Dudeney, A.W.L., Cheeseman, C.R., 2008. Controlled low-strength materials containing waste precipitates from mineral processing. Miner. Eng. 21, 252–263.

Brantley, S.L., 2003. Reaction Kinetics of Primary Rock-forming Minerals under Ambient Conditions. Treatise Geochem. 5, 73-117.

Cressey, G., Cressey, B.A., Wicks, F.J., 2008. The significance of the aluminium content of a lizardite at the nanoscale: the role of clinochlore as an aluminium sink. Mineralogical Magazine, 72, 3, 817-825.

Dahlin, C., O'Connor, W.K., Nilsen, D.N, Rush, G.E., Walters R.P. and Turner, P.C., 2000. A Method for Permanent CO_2 Mineral Carbonation. 17th Annual International Pittsburgh Coal Conference, September 11-15. DOE/ARC-2000-012.

Eloneva, S., Said, A., Fogelholm K.J. and Zevenhoven, R., 2012. Preliminary assessment of a method utilizing carbon dioxide and steelmaking slags to produce precipitated calcium carbonate. Appl. Energ. 90, 329–334.

Fabian, M., Shopska, M., Paneva, D., Kadinov, G., Kostova, N., Turianicova, E., Briančin, J., Mitov, I., Kleiv, R.A., Balazˇ, P., 2010. The influence of attrition milling on carbon dioxide sequestration on magnesium–iron silicate, Miner. Eng. 23, 616–620.

Fedoročková, A., Hreus, M., Raschman, P., Sučik, G., 2012. Dissolution of magnesium from calcined serpentinite in hydrochloric acid, Miner. Eng. 32, 1–4.

Fuchs, Y., Lineres J., and Mellini, M., 1998. Mössbauer and infrared spectrometry of lizardite 1T from Monte Fico, Elba. Phys. Chem. Min. 26, 111-115.

Gerdemann, S.J., O'Connor, W.K., Dahlin, D.C., Penner, L.R., Rush, H., 2007. Ex Situ Aqueous Mineral Carbonation, Environ. Sci. Technol. 41, 2587-2593.

Hitch, M., Dipple, G.M., 2012. Economic feasibility and sensitivity analysis of integrating industrial-scale mineral carbonation into mining operations. Miner. Eng. 39, 268–275.

Huijgen, W.J.J., Ruijg, G.J., Comans R.N.J. and Witkamp G.J., 2006. Energy consumption and net CO_2 sequestration of aqueous mineral carbonation, Ind. Eng. Res. 45, 9184-9194.

IPCC 2005, Special Report on Carbon Dioxide Capture and Storage. Metz B, Davidson O, de Coninck HC, Loos M and Meyer LA (Eds). Cambridge University Press, Cambridge, UK, p. 431.

Kodama, S., Nishimoto, T., Yamamoto, N., Yogo, K., Yamada, K., 2008. Development of a new pH-swing CO_2 mineralization process with a recyclable reaction solution. Energy 33, 776–784.

Lackner, K.S., Duby, P.F., Yegulalp, T., Krevor, S., Graves, C., 2008. TRP 9957 - Integrating Steel Production with Mineral Carbon Sequestration, May 2008, No. DE-FC36-97ID13554.

Liu, K., Chen, Q., Hu, H., Yin, Z., Wu, B., 2010. Pressure acid leaching of a Chinese laterite ore containing mainly maghemite and magnetite. Hydrometallurgy 104, 32-38.

Loring, J.S., Thompson, C.T., Wang, Z., Joly, A.G., Sklarew, D.S., Schaef, T.H., Ilton, E.S., Rosso K.M. and Felmy, A.R., 2011. In Situ Infrared Spectroscopic Study of Forsterite Carbonation in Wet Supercritical CO_2, Environ. Sci. Technol. 45, 6204–6210.

Maltman, A.J., 1977. Serpentinites and related rocks of Anglesey. Geological Journal, 12, 113-128.

McKelvy, M.K., Chizmeshya, A.V.G., Diefenbacher, J., Barat, H., and Wolf, G., 2004. Exploration of the Role of Heat Activation in Enhancing Serpentine Carbon Sequestration Reactions, Environ. Sci. Technol. 38, 6897-6903.

Mellini, M., Fuchs, Y., Viti, C., Lemaire C. and Lineres, J., 2002. Insights into the antigorite structure from Mössbauer and FTIR spectroscopies. Eur. J. Mineral. 14, 97-104.

Musić, S., Filipović-Vinceković N. and Sekovanić, L., 2011. Precipitation of amorphous SiO_2 particles and their properties, Braz. J. Chem. Eng. 28, 89 – 94.

Nduagu, E., Björklöf, T., Fagerlund, J., Wärnå, J., Geerlings, H., Zevenhoven, R., 2012a. Production of magnesium hydroxide from magnesium silicate for the purpose of CO_2 mineralisation – Part 1: Application to Finnish serpentinite. Miner. Eng. 30, 75–86.

Nduagu, E., Björklöf, T., Fagerlund, J., Mäkilä, E., Salonen, J., Geerlings, H., Zevenhoven, R., 2012b. Production of magnesium hydroxide from magnesium silicate for the purpose of CO_2 mineralization – Part 2: Mg extraction modeling and application to different Mg silicate rocks. Miner. Eng. 30, 87–94.

Nelson, M.C., 2004. Carbon Dioxide Sequestration by Mechanochemical Carbonation of Mineral Silicates, DE-FG26-99NT41547.

O'Connor, W.K., Dahlin, D.C., Rush, S G.E., Gerdermann, J., Penner, L.R., Nilsen, D.N., 2005. Aqueous Mineral Carbonation, DOE/ARC-TR-04-002 (http://www.netl.doe.gov).

Park, A.H.A. and Fan, L.S., 2004. CO_2 mineral sequestration: physically activated dissolution of serpentine and pH swing process, Chem. Eng. Sci. 59, 5241-5247.

Pourghahramani, P., Forssberg, E., 2006. Microstructure characterization of mechanically activated hematite using XRD line broadening, Int. J. Miner. Process. 79, 106‑119.

Sanna, A., Dri, M., Hall, M.R., Maroto-Valer, M.M., 2012a. Waste Materials as a Potential Resource for Carbon Capture and Storage by Mineralisation (CCSM) in the UK Context, Appl. Energ. 99, 545-554.

Sanna, A., Hall, M.R., Maroto-Valer, M.M., 2012b. A review of post-processing pathways in carbon capture and storage by mineralisation, Energ. Environ. Sci. 5, 7781-7796.

Sanna, A., Dri, M., Wang, X., Hall, M.R., Maroto-Valer, M.M., 2012c. Micro-silica for high-end application from carbon capture and storage by mineralisation, Key. Eng. Mat. 517, 737-744.

Sanna, A., Dri, M., Wang, X., Hall, M.R., Maroto-Valer, M.M., 2012d. Optimisation of

carbon capture and storage by pH swing aqueous mineralisation in presence of ammonium salts mixture, Fuel (http://dx.doi.org/10.1016/j.fuel.2012.08.014).

Seifritz, W., 1990. CO_2 disposal by means of silicates. Nature 345, 486.

Shoval, S., Ginott Y. and Nathan, Y., 1991. A new method for measuring the crystallinity index of quartz by infrared spectroscopy. Mineral. Mag. 55, 579-582.

Teir, S., Eloneva, S., Fogelholm J. and Zevenhoven, R., 2009. Appl. Energ. 86, 214–218.

Tromans, D., Meech, J.A., 2001. Enhanced dissolution of minerals: stored energy, amorphism and mechanical activation. Miner. Eng. 14, 1359‑1377.

Vardar, E., Eric, R.H., Letowski, F.K., 1994. Acid leaching of chromite. Miner. Eng. 7, 605-617.

Vogeli, J., Reid, D.L., Becker, M., Broadhurst, J., Franzidis, J.P., 2011. Investigation of the potential for mineral carbonation of PGM tailings in South Africa, Miner. Eng. 24, 1348–1356.

Wang, X. and Maroto-Valer, M.M., 2011a. Dissolution of serpentine using recyclable ammonium salts for CO_2 mineral carbonation, Fuel 90, 1229–1237.

Wang, X. and Maroto-Valer, M.M., 2011b. Integration of CO_2 Capture and Mineral Carbonation by using Recyclable Ammonium Salts, ChemSusChem 4, 1291-1300.

Wang, X. and Maroto-Valer, M.M., 2013. Optimization of carbon dioxide capture and storage with mineralisation using recyclable ammonium salts, Energy
http://dx.doi.org/10.1016/j.energy.2013.01.021

White, C., 2003. Mineral Carbonation Feasibility Study. Presentation at the Mineral Sequestration Working Group Review, National Energy Technology Laboratory, June 4, 2003, 626 Cochrans Mill Road, Pittsburgh, PA 15236-0940, USA, p.16-47.

List of Figures

List of Tables

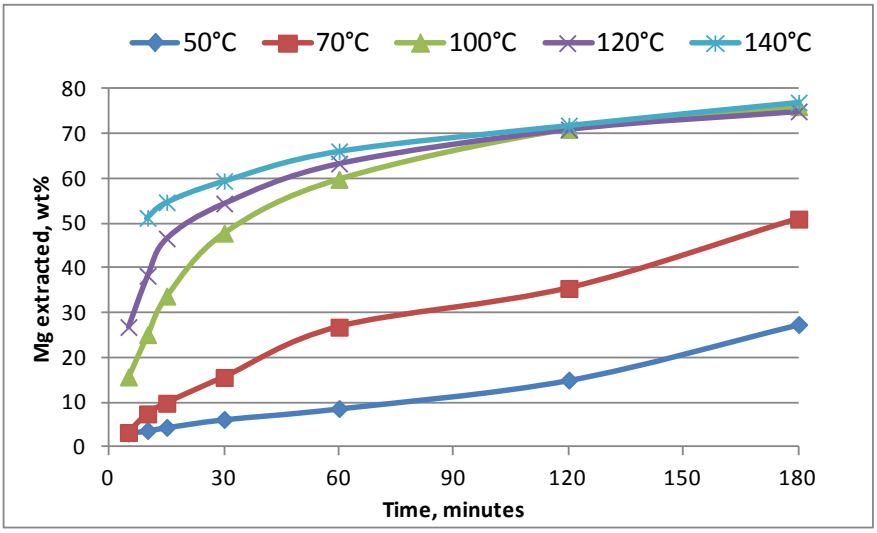

Figure 1. Effect of temperature and time on Mg extraction from serpentinised lherzolite.

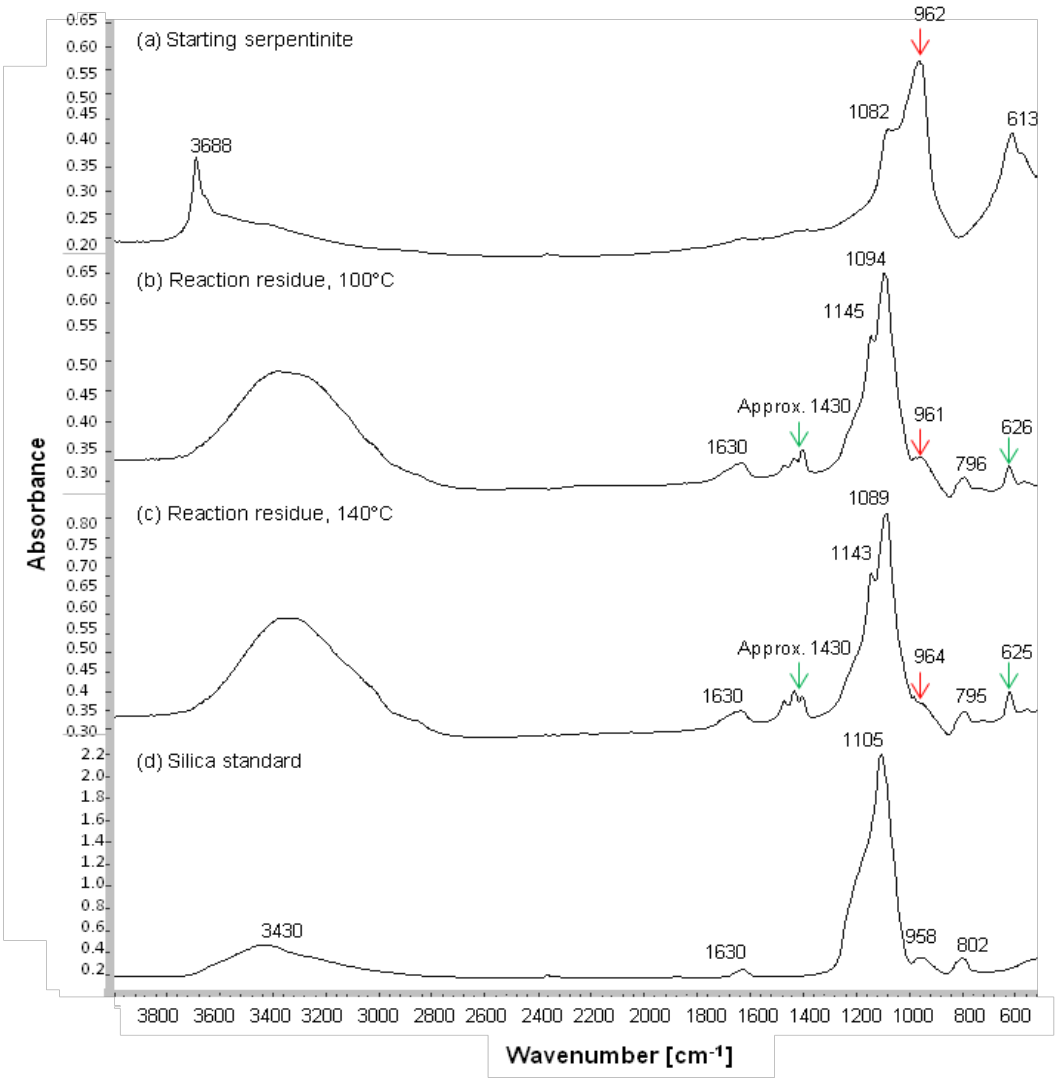

Figure 2. FTIR plot of (a) starting serpentinite, (b) dissolution residue obtained at 100°C, (c) dissolution residue obtained at 140°C, (d) silica standard.

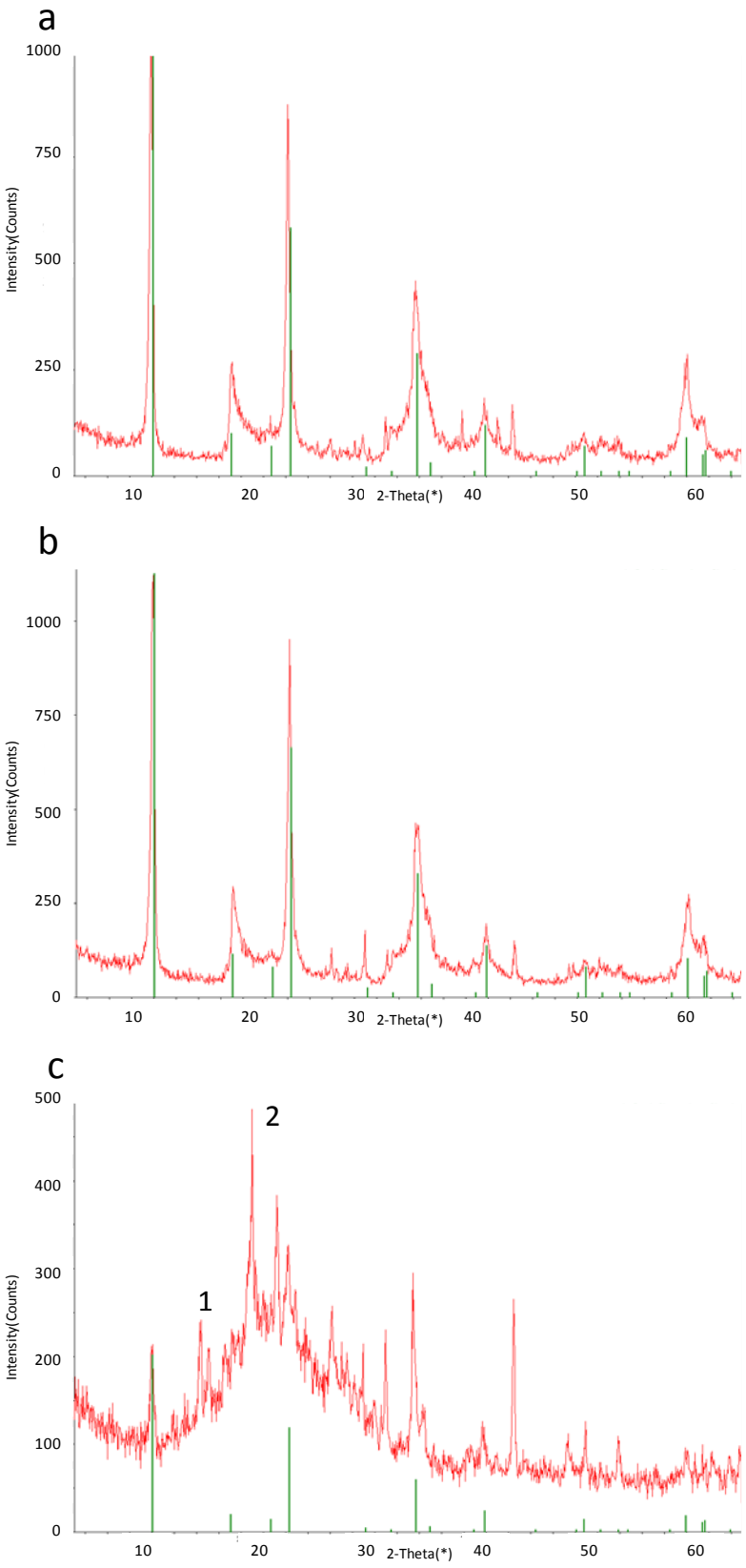

Figure 3. XRD patterns of a) raw serpentine, b) dissolution residue obtained at 100˚C, c) dissolution residue obtained at 140˚C. Green pattern represents Lizardite-1T; Peaks 1 and 2 represent magnesium sulphate salt (epsomite).

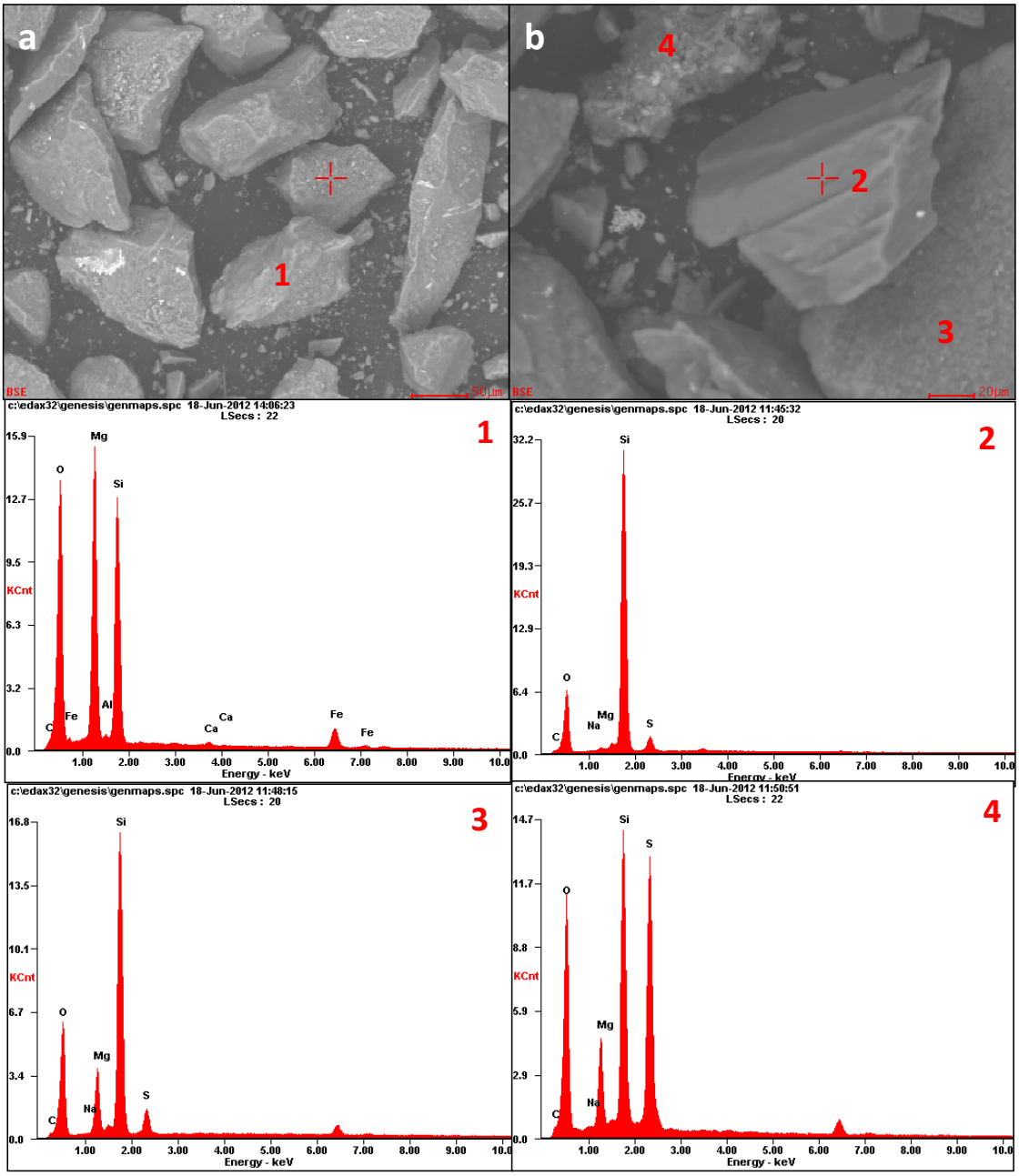

Figure 4. SEM images of the studied materials and the ED X-ray spectra from the particles indicated on the micrographs. A) raw serpentine, b) dissolution residue obtained at 140˚C.

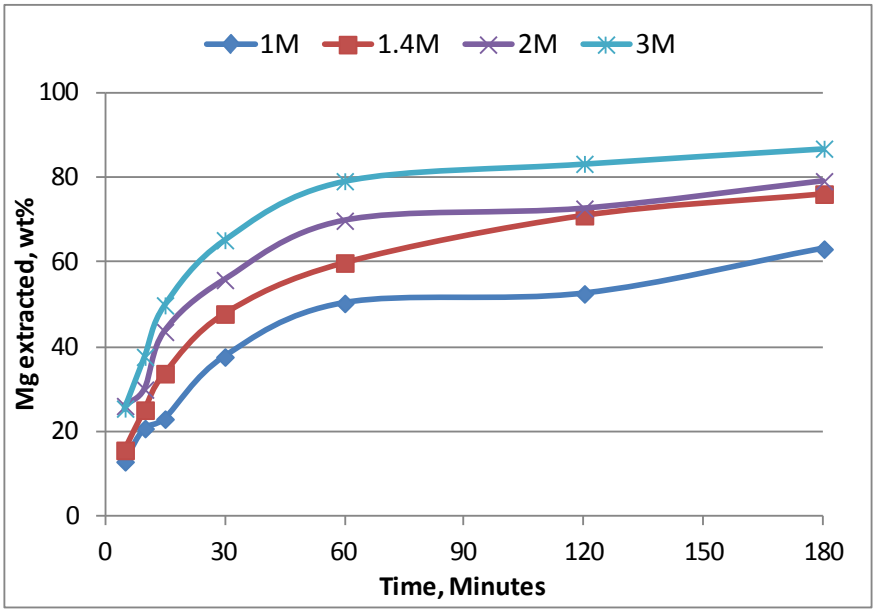

Figure 5. Effect of NH_4HSO_4 concentration and time on Mg extraction from serpentine.

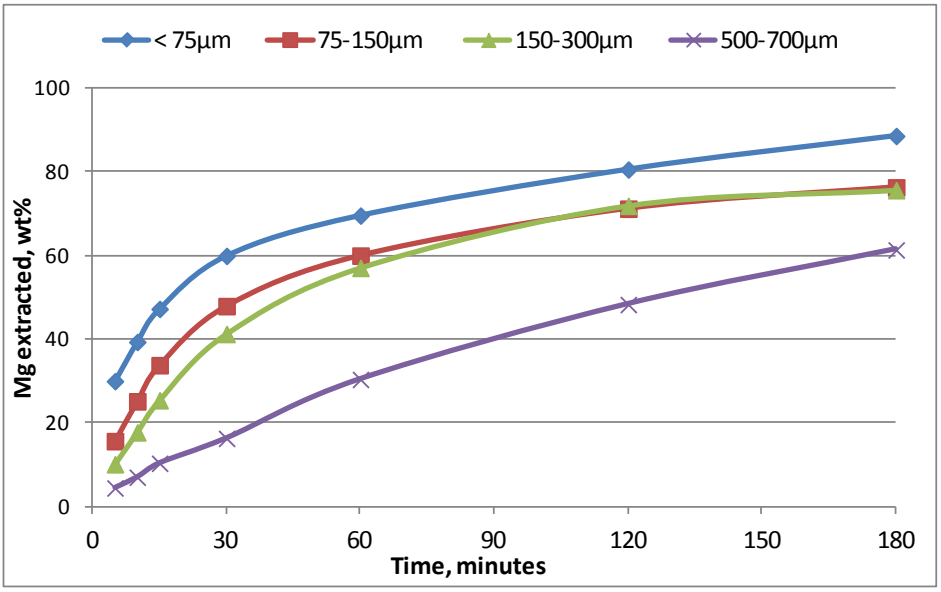

Figure 6. Effect of particle size and time on Mg extraction from serpentine sample (100°C, 50 g/l, 1.4 M NH_4HSO_4, 800 rpm).

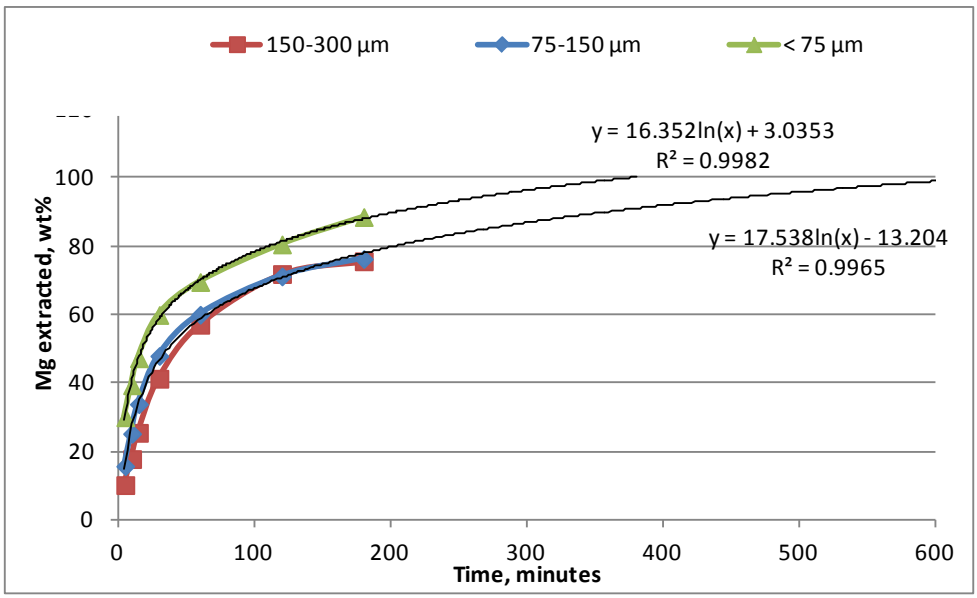

Figure 7. Forecast of the time required to extract 100% of Mg from the serpentine sample using different starting particle size (100 °C, 50 g/l, 1.4 M NH_4HSO_4, 800 rpm).

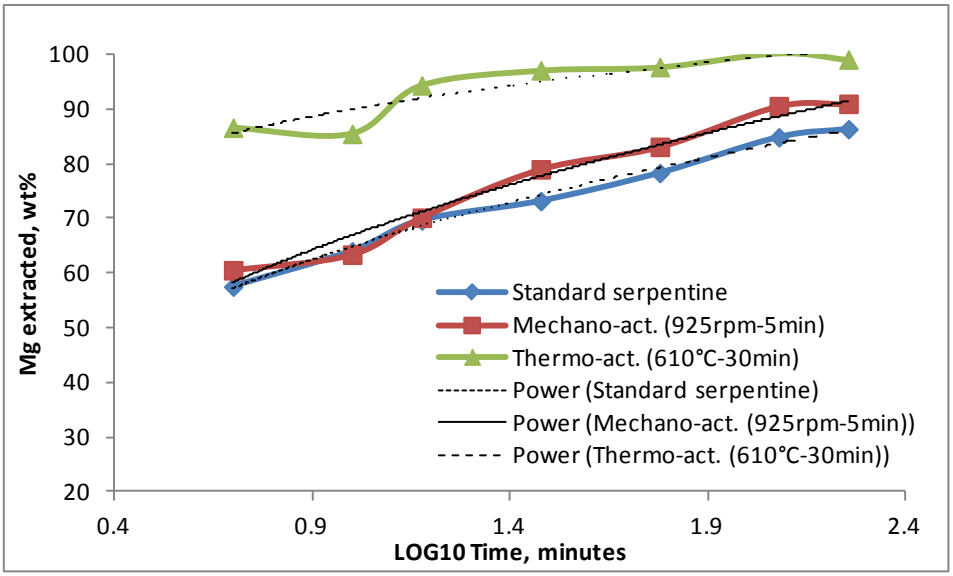

Figure 8. Mg leaching study from serpentine samples.

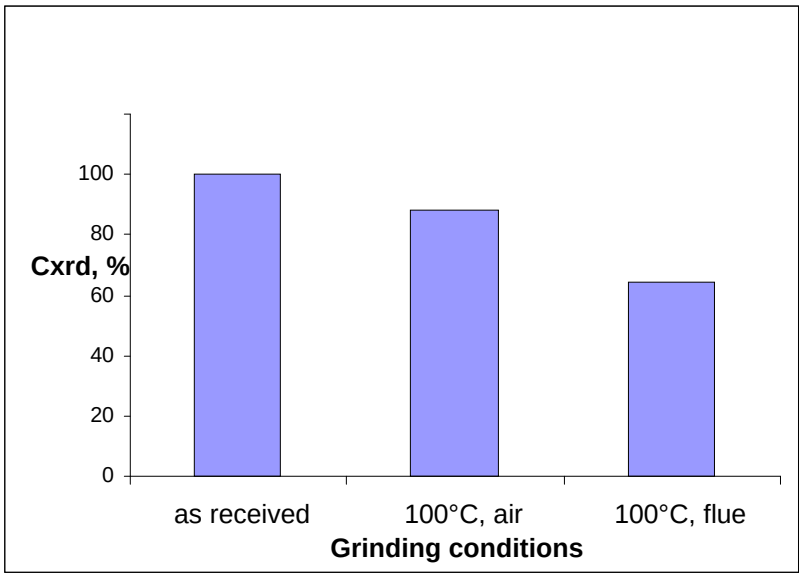

Figure 9. Crystalline phase (Cxrd) of serpentine lizardite-type samples ground at 925 rpm for 5 minutes in different environment.

Table1. Experimental summary.

Experiment type	**Experimental conditions**
Temperature	50°C, 70°C, 100°C, 120°C, 140°C
Pressure	Ambient pressure (1bar-4bar)
Solid/liquid ratio	25g/l, 50g/l, 100g/l
Particle size	<75µm, 75-150µm, 150-300µm, 500-700µm
Additive concentration	1M, 1.4M, 2M, 2.8M, 3M (NH_4HSO_4)
Thermo-activation	610°C for 30 minutes, in presence of air and flue gas (10%CO_2)
Mechanical-activation	409rpm, 620rpm, 925rpm, 5-10-60 min, in presence of air and flue gas (10%CO_2)

Table 2. Effect of NH_4HSO_4 concentration on Fe extraction at 100°C and 50g/l.

	Fe, wt%			
Time, min	**1M**	**1.4M**	**2M**	**3M**
5	9.0	11.5	31.1	37.7
10	14.3	17.8	38.1	54.3
15	15.1	23.5	54.7	71.2
30	23.9	32.6	69.7	94.2
60	31.2	40.5	87.9	100.0
120	32.0	48.3	93.3	100.0
180	37.9	51.8	100.0	100.0

Table 3. Effect of particle size and time on Fe extraction from serpentine sample (100 °C, 50 g/l, 1.4 M NH_4HSO_4, 800 rpm).

	Fe, wt%		
Time, min	**< 75µm**	**75-150µm**	**150-300µm**
5	43.14	11.54	7.05
10	55.73	17.81	12.03
15	65.96	23.53	16.95
30	82.51	32.58	26.90
60	94.21	40.50	36.88
120	100.00	48.34	46.64
180	/	51.78	49.42

Table 4. Effect of grinding speed and duration on particles size distribution and energy consumption.

Grinding speed and time	Particle size distribution (wt%)			Energy consumption
(rpm-min)	< 250 µm	< 150 µm	< 75 µm	(kWh/t)
314-60	34.5	27.9	17.4	69.5
409-60	86.9	48.8	43.5	86.9
620-10	55.6	50.1	37.6	22.7
920-5	55	50.6	32.1	16.2
920-10	88.1	87.4	37.7	33.2

Table 5. Element abundance (wt%) in solution at different pH during pH swing process.

	Initial	pH 3	pH 6	pH 6.5	pH 7
Element	**wt%**	**wt%**	**wt%**	**wt%**	**wt%**
Fe	100.0	89.2	25.4	14.6	6.4
Al	100.0	93.4	12.5	2.4	0.2
Ni	100.0	100.0	84.4	71.6	72.9
Mn	100.0	100.1	100.8	94.4	83.9
Mg	100	99	98.5	98	97.8

Table 6. Abundance of Mg in solution (wt%) during carbonation reaction.

Time, min	Mg in solution, wt%
0	97.8
5	30.5
10	23.4
15	19.6
30	12.3
60	6.2